Scripta METALLURGICA et MATERIALIA
Vol. 30, pp. 429-434, 1994
Printed in the U.S.A.
Pergamon Press Ltd.
All rights reserved

QUASI-STATIC CONSTITUTIVE BEHAVIOR OF $Zr_{41.25}Ti_{13.75}Ni_{10}Cu_{12.5}Be_{22.5}$ BULK AMORPHOUS ALLOYS

H.A. Bruck, T. Christman, A.J. Rosakis, and W.L. Johnson
Div. of Eng. and App. Sci., Cal. Inst. Tech., Pasadena CA 91125

(Received August 25, 1993)
(Revised November 8, 1993)

1. Introduction

The mechanical behavior of amorphous metal alloys (a.k.a. metallic glasses) has been an area of intense research for many years because of the material's ultra-high strength and unique plastic mechanical behavior. The strength of amorphous alloys approaches theoretical limits while the mode of plastic deformation depends on temperature and strain rate. Various micromechanical models have been proposed to account for the mechanical behavior of amorphous alloys [1-7]. These models have spawned significant debate regarding their suitability for describing the observed mechanical properties. Some of these models have adapted descriptions of classical defects in polycrystalline materials to amorphous metal alloys [3-5]. However, developing consistent and unique definitions of defects in amorphous structures remains a topic of controversy because of the absence of long range order in these materials. In addition, there is only a limited amount of information available on the plastic deformation of bulk amorphous metal alloys in multi-axial stress states [8,9]. This information is necessary to critically assess the proposed micromechanical models.

Some insight into the micromechanisms of plastic deformation in amorphous alloys can be obtained by determining the yield surface. Kimura and Masumoto [8] conducted plastic flow experiments on $Pd_{77.5}Cu_6Si_{16.5}$ which suggested that amorphous alloys obey a von Mises yield criterion. Attempts by Donovan [9] to construct an experiment capable of producing a state of pure shear in notched bars of $Pd_{40}Ni_{40}P_{20}$ led to the conclusion that plastic flow in amorphous alloys may exhibit a sensitivity to normal stresses acting across the slip plane, which is best described using a Mohr-Coulomb type of yield criterion. Although Masumoto's and Donovan's experiments seem to support different criteria for yielding, experiments have yet to be performed on specimens of sufficient size to produce a well defined stress state during mechanical testing. The absence of such experiments is primarily due to the lack of availability of bulk amorphous alloys.

Cooling rate requirements have limited the size of amorphous specimens previously available for mechanical testing to cylindrical rods 2 mm or less in diameter. Recent metallurgical developments by Peker and Johnson [10] and the group of Inoue and Masumoto [11-13] have provided the opportunity to conduct mechanical tests on bulk amorphous alloys that can be cast as cylindrical rods up to 16 mm in diameter. In this paper, samples are machined from these alloys into "dogbone" specimens whose dimensions are large enough to insure a well defined stress state for tension and torsion testing. Strain gages are attached to the surface of the specimens to measure local deformations. The results are compared with previous experiments to determine an appropriate yield criterion for amorphous alloys.

2. Experimental Procedure

Rods of $Zr_{41.25}Ti_{13.75}Ni_{10}Cu_{12.5}Be_{22.5}$ were prepared by two casting methods. The first method

0956-716X/94 $6.00 + .00
Copyright (c) 1993 Pergamon Press Ltd.

involved injecting the molten alloys into copper molds with cylindrical cavities that are 2.5 and 3 mm in diameter. In the second method, the alloys were melted by induction heating in evacuated quartz tubes 7 mm in diameter, then quenched in water. Details of the alloy design and the casting procedures can be found in reference [10]. Periodically, discs approximately 250 mm thick were machined from the rods and placed in an Inel CPS-120 x-ray diffractometer to verify that the structure was amorphous.

For compression tests, specimens were machined from these rods with length to diameter (l/d) aspect ratios ranging from 1:2 to 2:1. The ends of the specimens were then mechanically polished with 600 grit grinding paper using a V-block to insure flat and parallel surfaces. By measuring the length of the specimen with a micrometer, the surfaces were found to be parallel within 3 μm. For tension and torsion tests, specimens were ground from the 7 mm rods into a "dogbone" geometry with dimensions proportional to ASTM standard E8-68 for tension testing. The exact dimensions of these test specimens can be seen in Figure 1.

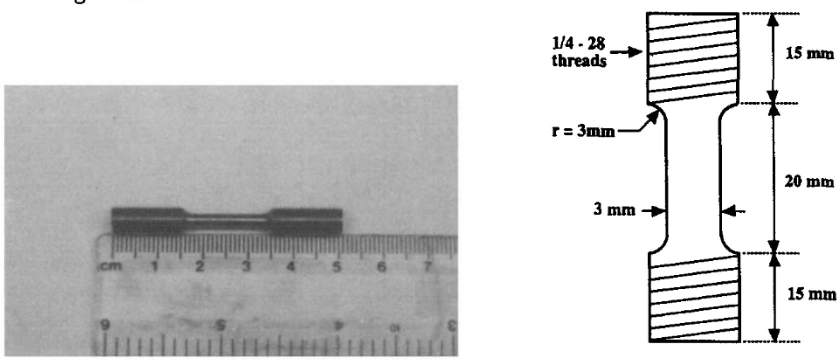

Figure 1. Sample pictures and geometry.

All mechanical testing was performed using an MTS 319.25 axial-torsional load frame. In the compression tests, specimens were placed between a pair of tungsten carbide inserts coated with "Molygraph Extreme Pressure Multi-Purpose" grease. The specimens were loaded in a special frame that was designed according to ASTM standard E9-67 to insure that the specimens experience only uniaxial loading. In the tension-torsion tests, the specimens were threaded into grips that were connected by U-joints to the load frame to reduce the bending moments transmitted to the specimen.

Compression and tension-torsion tests were conducted using constant crosshead velocities. The resulting strain rates varied from 10^{-4}/sec to 10^{-3}/sec. In the compression tests, strains were calculated using the crosshead displacement after correcting for the compliance of the load train. For the tension tests, a uniaxial strain gage from the Micromeasurements Group was used to obtain one-dimensional surface strains, while for the tension-torsion tests a rectangular strain gage rosette was used to obtain two-dimensional surface strains.

Elastic properties were measured by means of ultrasonic techniques on a 10 mm long section of 7 mm diameter rod whose ends were polished with the 600 grit grinding paper using the V-block. Two ultrasonic transducers were then placed on the ends of the rod. One transducer measured the dilitational wave speed while the other measured shear wave speeds. The elastic properties were then calculated using standard techniques [14]. The specimen's density was measured using the hydrostatic weighing technique with toluene as the working fluid.

3. Experimental Results

To determine the uniaxial compressive behavior, specimens were used with diameters of 2.5, 3 and 7 mm. The l/d aspect ratio for all specimens was approximately 3:2, which conforms to the ASTM

standard E9-89a for high strength materials. The yield stress for the 2.5 and 3 mm specimens was measured to be 1.93 ± 0.03 GPa, while for the 7 mm specimens it was measured to be 1.87 ± 0.03 GPa. The yield stress was defined as the stress at the plateau of the stress-strain curve. Typical stress-strain curves for each diameter can be seen in Figure 2. It shows that flow proceeds at a constant stress with some serrated features until failure occurs by localization. This is similar to the compressive yield behavior observed by previous researchers [15,16].

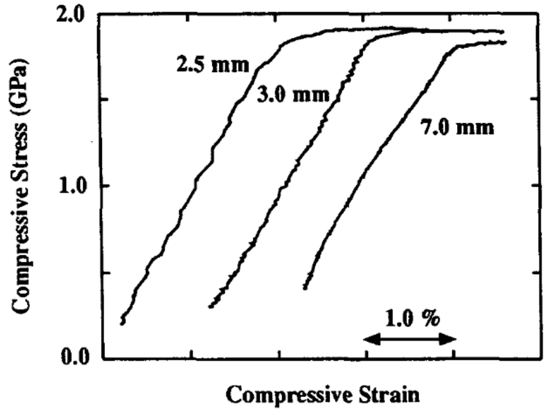

Figure 2. Compressive stress-strain curves.

Compression tests were also conducted on cylindrical samples with aspect ratios of approximately 3:4. The yield stress was measured at 2.12 ± 0.05 GPa. As aspect ratios are lowered, the triaxiality of the stress field increases [17]. Consequently, an increase in yield strength would be expected for materials whose flow is insensitive to hydrostatic pressure.

A typical tensile stress-strain curve can be seen in Figure 3. There appears to be no yielding before failure, which occurs by a localized shear mechanism. This observed deformation behavior is similar to that of Masumoto's specimens [8], but differs from measurements made previously on thin amorphous ribbons that appear to exhibit yielding before failure [16,18]. Consequently, the yield strength and the failure strength are considered identical and were measured to be 1.89 ± 0.03 GPa, which lies in the range of aforementioned compressive yield strengths.

The specimens used for the tension tests were also used in the torsion tests. The resulting stress-strain curve for a typical test can be seen in Figure 3. The shear stress can be related to the measured torsional moment, M_T, by balancing moments for an elastic-perfectly plastic rod as follows:

$$M_T = 2\pi\left\{\int_b^R \tau_y r^2 dr + \int_0^b \tau(r) r^2 dr\right\} \tag{1}$$

where R is the radius of the rod, b is the radial position for the plastic zone boundary, τ_y is the yield stress in shear, r is the radial position, and $\tau(r)$ is the elastic shear stress.

One can calculate the shear strain, $\gamma(r)$, from the deformation of the rod as follows:

$$\gamma(r) = \frac{\theta r}{L} \tag{2}$$

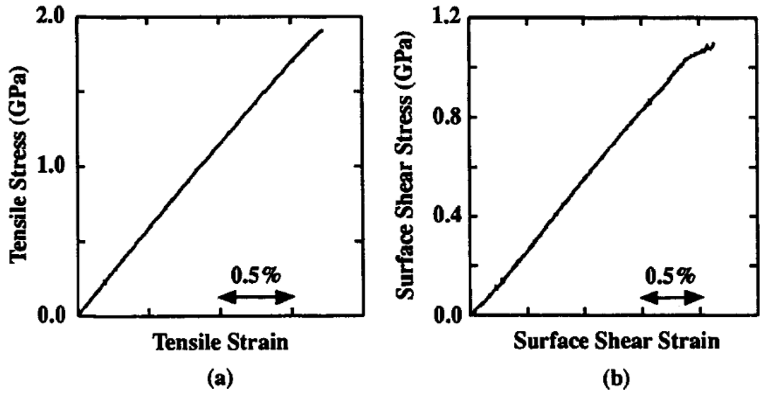

Figure 3. (a) Tension stress-strain curve. (b) Torsion stress-strain curve.

where θ is the angle of rotation imposed on the rod and L is the length of the rod. The shear strain can then be used to calculate the elastic shear stress ($\tau(r) = \mu\gamma(r)$). Rearranging these equations and calculating the integrals, one finds:

$$M_T = \pi\tau_o\left\{\frac{2}{3}R^3 - \frac{b^3}{6}\right\} \tag{3}$$

where τ_o is the shear stress at the surface of the rod which is equal to $\mu\theta R/L$ when the rod is fully elastic and equal to τ_y after yielding has occurred.

From equation (2), the failure strain, γ_f, on the outer surface can also be used to predict the radial position of the plastic zone boundary at failure, b_f as follows:

$$b_f = \frac{\gamma_y}{\gamma_f}R \tag{4}$$

where γ_y is the strain at which yielding is initiated on the outer surface. From Figure 3, it appears that yielding is initiated at $\gamma_y \simeq 0.019$ and failure occurs at $\gamma_f \simeq 0.021$. Therefore, for a rod 1.5 mm in radius, the radial position of the plastic zone boundary at failure is approximately 1.36 mm.

Because of the limited extent of yielding in the torsional experiments ($b \simeq 0.9R$), the shear stress at the surface of the rod was calculated neglecting yielding in equation (1) as follows:

$$\tau(R) = 2M_T\pi^{-1}R^{-3} \tag{5}$$

The shear stress increases monotonically in Figure 3 and does not reach a plateau value because of the limited ductility and the inhomogeneous torsional stress state. The shear yield behavior has serrated features similar to those observed in the compressive yield behavior. The shear yield strength was taken to be the point at which the shear response deviates significantly from linearity, 1.03 GPa. This is the yield strength predicted by a Von Mises criterion using a tensile or compressive yield strength of 1.78 GPa, approximately 6% below the reported yield strengths.

The extent of yielding at failure in an elastic-perfectly plastic rod under torsional load can also be calculated from equation (3) as follows:

$$b^3 = 4R^3 - 6M_T\pi^{-1}\tau_y{}^{-1} \tag{6}$$

Plugging equation (5) into equation (6) yields:

$$b^3 = R^3(4 - 3\tau(R)\tau_y{}^{-1}) \tag{7}$$

From Figure 3, the failure stress in shear is 1.10 GPa, which results in the radial position of the plastic zone boundary at failure being 1.39 mm. The consistency in predicting the plastic zone boundary based on equations (7) and (4) supports the assumption of elastic-perfectly plastic constitutive behavior.

An optical micrograph taken of the torsional fracture surface, Figure 4, reveals a thin band near the outer surface. The band terminates at a radial position of approximately 1.35 mm, equivalent to the previous plastic zone calculations. Detailed investigations of the failure process are required to directly correlate this fractographic feature with prior plastic deformation.

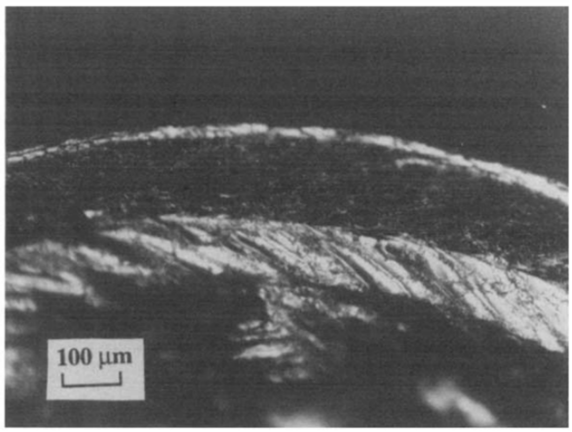

Figure 4. Torsional fracture surface.

The density of the amorphous Zr alloy was 6.11 ± 0.01 g/cm^3. The shear wave speed was 2337 m/s ± 13 m/s and the longitudinal wave speed was 4913 ± 25 m/s. The Young's modulus and Poisson's ratio were 93 ± 1 GPa and 0.387 ± 0.003 respectively. The amorphous material is slightly softer than crystalline Zr, which has a Young's modulus of 98-99 GPa and a Poisson's ratio of 0.35-0.38 at room temperature [19,20] .

4. Discussion

For isotropic, pressure insensitive solids, the Von Mises yield criterion is as follows [14]:

$$(\sigma_1 - \sigma_2)^2 + (\sigma_1 - \sigma_2)^2 + (\sigma_2 - \sigma_3)^2 = 6k^2 \tag{8}$$

where σ_1, σ_2, and σ_3 are the principal stresses and k is a constant equal to the yield stress in shear. From this criterion, it is predicted that the compressive and tensile yield stresses are equivalent, while the ratio of these stresses to the shear yield stress should be 1.73. The measured values of compressive and tensile yield stress are approximately equivalent, while the ratio of these yield stresses to the shear yield stress is 1.84.

For plane strain compression, $\sigma_y = \sigma_o/(1-\nu+\nu^2)^{1/2}$, where σ_y is the yield stress in plane strain compression and σ_o is the yield stress in uniaxial compression. Using the value of Poisson's ratio, ν, from the ultrasonics measurements, σ_y should be $1.15\sigma_o$. As the aspect ratio for the compression test specimens decreased, the yield stress increased from an average of 1.90 GPa to 2.12 GPa. The resulting ratio of the two yield stresses is 1.12, which approaches the Von Mises prediction. These results support the conclusion that the Zr alloy obeys the Von Mises yield criterion.

Importantly, Kimura and Masumoto [8] have observed similar relationships between aspect ratios and yield stress, Donovan [9] reported no change in yield stress as aspect ratios decreased. Donovan attributes this behavior to a lack of frictional constraints on the ends of his test specimens. Without friction, a triaxial stress field can not be established and the plane strain conditions can not be approached. To simulate plane strain conditions, Donovan used a testing configuration proposed by Watts and Ford [21]. His experimental results indicated no difference between uniaxial and plane strain yield strengths, contrary to the results reported here. It is not clear whether the contradictions between the present results and those of Donovan are due to differences in materials or experimental methods.

5. Summary

Mechanical tests have been performed on bulk amorphous metal alloys to determine their constitutive behavior. Based on the experimental results, it appears that amorphous metal alloys obey a Von Mises yield criterion. This result has implications in determining the micromechanisms of plastic deformation in these materials.

Acknowldgement

The authors acknowledge partial support of this work by the Department of Energy under grant DE-FG03-86ER45242.

References

1. F. Spaepen, Acta Met. 25, 407 (1977).
2. A.S. Argon, Acta Met. 27, 47 (1979).
3. J.J. Gilman, J. App. Phys. 46, 1625 (1975).
4. J.C.M. Li, in "Rapidly Quenched Metals 4" (ed. T. Masumoto and S. Suzuki; Japan Instute of Metals) 2, 1335 (1981).
5. D.R. Nelson, Phys. Rev. B 28, 5515 (1983).
6. D. Srolovitz, V. Vitek, and T. Egami, Acta Met. 31, 335 (1983).
7. S. Takeuchi and K. Maeda, Key Engineering Materials, Vol. 13-15, 749 (1987).
8. H. Kimura and T. Masumoto, in "Amorphous Metallic Alloys" (edited by F. Luborsky; Butterworths, London), 187 (1983).
9. P.E. Donovan, Acta Met. 37, 445 (1989).
10. A. Peker and W.L. Johnson, App. Phys. Lett. 63, 2342 (1993).
11. A. Inoue, T. Zhang and T. Masumoto, Mat. Trans. Japan Institute of Metals 31, 425 (1990).
12. T. Zhang, A. Inoue, and T. Masumoto, Mat. Trans. Japan Institute of Metals 32, 1005 (1991).
13. A. Inoue, Y. Nakamura, N. Nishiyama, and T. Masumoto, Mat. Trans. Japan Institute of Metals 33, 937 (1992).
14. L.E. Malvern, in "Introduction to the Mechanics of a Continuous Medium", (Prentice-Hall Inc., Englewood Cliffs, NJ) (1969).
15. P.E. Donovan, Mat. Sci. Eng. 98, 487 (1988).
16. C.A. Pampillo and H.S. Chen, Mat. Sci. and Eng. 13, 181 (1974).
17. S. Peng and A.M. Johnson, Int. J. of Rock Mech. and Minerals Sci. 9, 37 (1972).
18. H.J. Leamy, H.S. Chen, and T.T. Wang, Met. Trans. 3, 699 (1972).
19. ASM Metals Handbook Desk Edition (edited by H.E. Boyer and T.L. Gail; American Society for Metals, Metals Park, Ohio), 14.13 (1985).
20. Smithells Metals Reference Book (edited by E.A. Brandes and E.B. Brook; Butterworth-Heinemann, Linacre House, Jordan Hill, Oxford), 15-3 (1992).
21. A.B. Watts and H. Ford, Proc. Inst. Mech. Eng. B 1, 448 (1952).